

Metabolomic insights into the function and nutritional quality of special rice

Di Cui^{a,b}, Zichao Zhu^c, Soon-Wook Kwon^d, Joohyun Lee^e, Mingmao Sun^f, Xiaoding Ma^{a,b}, Chutao Wang^c, Bing Han^{a,b}, Xianying Li^{c,*}, Longzhi Han^{a,b,**}

^a State Key Laboratory of Crop Gene Resources and Breeding, Institute of Crop Sciences, Chinese Academy of Agricultural Sciences, Beijing 100081, China

^b Key Laboratory of Grain Crop Genetic Resources Evaluation and Utilization Ministry of Agriculture and Rural Affairs, Institute of Crop Sciences, Chinese Academy of Agricultural Sciences, Beijing 100081, China

^c Chongqing Academy of Agricultural Sciences, Chongqing 401329, China

^d Department of Plant Bioscience, Pusan National University, Miryang, 50463, Republic of Korea

^e Department of Crop Science, Konkuk University, Seoul 05029, Republic of Korea

^f Biological Engineering Research and Development Center, Weifang University of Science and Technology, Shouguang, Shandong 262700, China

ARTICLE INFO

Keywords:

Special rice
Metabolomic analysis
Differential metabolites
Nutritional quality
γ-Aminobutyric acid
Flavonoids
Phenolic acids

ABSTRACT

The global demand for nutrient-rich functional rice is rapidly increasing. However, the metabolic mechanisms underlying the high-nutrient functionality of special rice remain inadequately understood. In this study, we developed 26 novel special rice accessions. Using a widely targeted metabolomics approach, we identified and classified 1347 metabolites. The metabolite profiles of these accessions exhibited substantial differentiation, with 204–629 differentially accumulated metabolites identified. Notably, pigmented giant embryo glutinous (PGE) rice integrated a diverse array of bioactive compounds and nutrients from pigmented rice and giant embryo glutinous rice. It was particularly enriched in γ-aminobutyric acid (GABA), flavonoids, phenolic acids, alkaloids, and other physiologically active substances. Key metabolic pathways (including the biosynthesis of flavone, flavonol, and flavonoid) were significantly enriched in differential metabolites between white/glutinous and PGE rice. These findings provide a comprehensive understanding of the metabolite profiles of special rice varieties and offer valuable insights for breeding future high-nutrient functional rice.

1. Introduction

Rice is a staple food crop worldwide, rich in essential nutrients and trace elements. Functional rice, often termed special rice, possesses a unique genetic composition, resulting in higher concentrations of bioactive components compared to conventional rice varieties, such as flavonoids, phenols, organic acids, terpenoids and alkaloids, etc. These bioactive compounds not only meet dietary requirements but also support human health by regulating physiological functions and metabolism.

Previous studies have shown that pigmented rice varieties are abundant in essential amino acids, dietary fibers, anthocyanins, phenolic compounds, functional lipids, minerals and vitamins, etc. (Mau, Lee, Chen, & Lin, 2017; Tang, Cai, & Xu, 2016). Owing to these

properties, pigmented rice is often referred to as “medicinal rice,” with the potential to enhance immunity and improve overall health. In recent years, giant embryo rice which is rich in γ-aminobutyric acid (GABA) has attracted widespread global interest due to its high nutritional value. GABA, an inhibitory neurotransmitter, has been associated with various neurological disorders, such as Huntington’s/Parkinson’s/Alzheimer’s disease, epilepsy, tetanus syndrome, and schizophrenia. It holds therapeutic potential to mitigate these conditions (Battaglioli, Liu, & Martin, 2003). Beyond its neurological benefits, GABA supports liver and kidney function, promotes insulin secretion, and shows promise in diabetes management (Huang et al., 2014). Additionally, it has been shown to reduce blood pressure, prevent arteriosclerosis, regulate arrhythmia, and exhibit anti-fatigue and anti-aging effects.

Countries where rice is a dietary staple, including Japan, South

* Corresponding author.

** Corresponding author at: State Key Laboratory of Crop Gene Resources and Breeding, Institute of Crop Sciences, Chinese Academy of Agricultural Sciences, Beijing 100081, China.

E-mail addresses: cqseed@126.com (X. Li), hanlongzhi@caas.cn (L. Han).

<https://doi.org/10.1016/j.fochx.2025.102890>

Received 22 January 2025; Received in revised form 30 July 2025; Accepted 5 August 2025

Available online 8 August 2025

2590-1575/© 2025 The Author(s). Published by Elsevier Ltd. This is an open access article under the CC BY-NC-ND license (<http://creativecommons.org/licenses/by-nc-nd/4.0/>).

Korea, and China, have prioritized breeding high-GABA rice varieties. In Japan, several giant embryo rice varieties, such as “Haiminori,” “Beihai 269,” and “Oyu 359,” have been developed with elevated GABA levels, catering to hypertensive patients (Hu, 2003; Su, Wan, Zhai, & Wan, 2007). Similarly, in South Korea, mutations induced in the japonica rice “Hwachungbyeol” have yielded giant embryo rice mutants enriched in protein, fat, lysine, tocopherol, and vitamin B1 (Kim, Heu, & Park, 1991; Koh, Heu, & McCouch, 1996). In China, “Jupeigeng 1” (7.8 mg/100 g GABA) was bred using 95–20 as the male parent and Jupeidaohuaqing M-2-565-11-3-B as the female parent (Hu & Hu, 2021). Additionally, Zhang et al. (2019) crossed Heishuai with Jupei 1/Zao 25 to produce Heizhenzhu, a variety with high GABA content and blood pressure-lowering properties.

As living standards and consumer preferences evolve, the demand for high-nutrient functional rice grows. Cultivating such rice varieties offers immense economic potential and promising applications. In China, numerous functional rice varieties have been developed using methods like crossbreeding, mutation breeding, and genetic introduction. These varieties, including “Yishendao 1” (low gluten), “Kangdun 1” (low water-soluble protein), “Yuehang 1” (selenium-rich), “Heiyouzhan 3” (iron-rich), and “Gongmi 3” (high resistant starch), demonstrate enhanced health benefits (Hu & Hu, 2021; Liu, Jiang, & Liu, 2005). Despite these advancements, the metabolic mechanisms underlying the high-nutrient functionality of special rice remain inadequately explored. Nowadays, widely targeted metabolite profiling which employs high-throughput approaches to explore the metabolome of plant-derived products, resulting in an accurate qualitative and quantitative identification of metabolites have been successfully used in the studies of function and nutritional quality of plants (Zhang, Cui, Ma, Han, & Han, 2023; Zhao et al., 2024).

In this study, we used a UPLC-MS/MS-based widely targeted metabolomics approach to comprehensively analyze the metabolite profiles of 26 developed novel special rice accessions to identify differential metabolites, elucidate key metabolic pathways, and characterize bioactive compound variations. Our findings offer a foundation for the breeding of new high-nutrient functional rice varieties.

2. Material and methods

2.1. Development of novel special rice

We developed the novel special rice germplasms from a single cross between Heinuomi × Jupeixiangnuo by crossbreeding and pedigree selection. Specifically, trait segregations occurred in the F₂ and we strictly selected the lines by evaluating the appearance of brown rice for each generation from F₂. Finally, 26 novel rice accessions containing one or more special traits such as colored seed coat, giant embryo, and

glutinous characteristics were obtained in F₁₀. These included six black giant embryo glutinous rice (BGRGE), six red giant embryo glutinous rice (RGRGE), four giant embryo glutinous rice (GRGE), three black rice (BR), four red rice (RR) and three glutinous rice (GR). Additionally, three white rice (WR) accessions from the same cross between Heinuomi × Jupeixiangnuo but the special traits of the appearance of brown rice were not included were selected as controls (Fig. 1).

2.2. Field cultivation of rice materials

A total of 29 rice germplasms were planted in an experimental farm, Chinese Academy of Agricultural Sciences, Beijing, China, during the same season under uniform conditions. The seeds of each plant were sown on April 20, 2022 and were transplanted on May 25, 2022, with a randomized block design. N, P (P₂O₅) and K (KCl) fertilizers were applied at 120 kg/hm², 60 kg/hm² and 112.5 kg/hm². Each plot was consisted of 5 rows with 20 plants per row, which spaced 15 cm apart between plants, with 25-cm spacing between rows. After maturity, all plants were harvested and threshed on September 22, 2022. After sun-drying, when the moisture content reached 10–11 % by sun exposure, grains were kept at 4 °C in dark space for 10 months until being used.

2.3. Identification of quality traits of brown rice

According to the Chinese agricultural industry standard “NY/T 83-2017 Determination of rice quality.” Grains was dehulled to obtain brown rice using a dehulling machine and the residual grains in the brown rice were removed. Brown rice quality traits were assessed using established standards and methods. Length, width, and thickness were measured with a Wanshen SC-G seed rice appearance quality analyzer. Embryo length was determined using a vernier caliper, with measurements taken from 10 grains per accession. The average weight of 1000 full brown rice grains was calculated from two replicates. Head rice rate were measured following the Chinese agricultural industry standard “NY/T 83-2017 Determination of rice quality.” Approximately 10 g of brown rice was milled for 1 min using a rice mill to achieve the national standard grade three level of milling precision. The milled rice was then sieved using a grain sieve with a 1.5 mm opening to separate the bran and husk. A milled rice sample was thoroughly mixed, and a sample ranging from 10 g to 35 g was taken using a sample divider. Finally, The weight of the head rice (HR) and the total weight of the milled rice sample (MR) were then measured using a balance with an accuracy of 0.01 g. The head rice rate (HRR) was calculated according to the following formula: $HRR (\%) = HR/MR \times 100$.

Alkali spreading value were determined following the Chinese agricultural industry standard “NY/T 83-2017 Determination of rice quality.” Six randomly selected mature and intact grains of milled rice

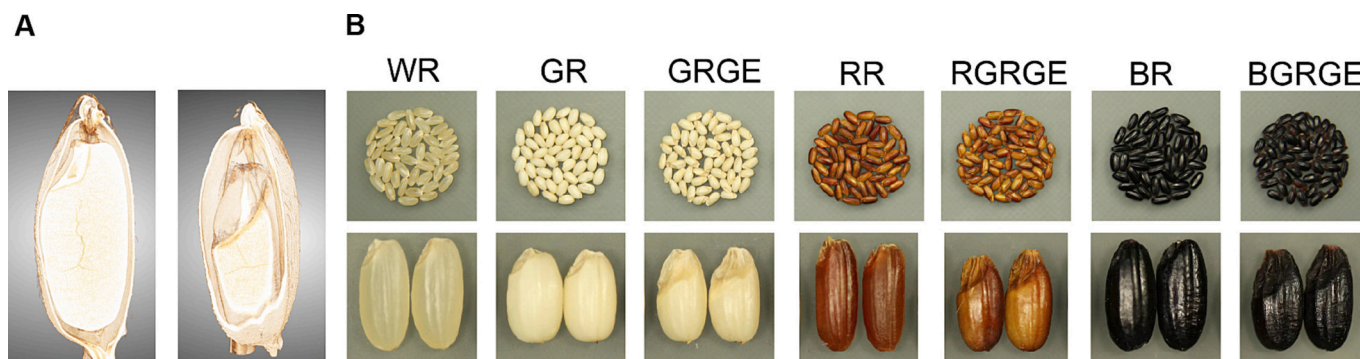


Fig. 1. High-resolution CT scans and photographs of brown rice varieties. (A) High-resolution CT scans of glutinous rice (left) and giant embryo glutinous rice (right). (B) Photographs of brown rice varieties. WR, white rice; GR, glutinous rice; GRGE, giant embryo glutinous rice; RR, red rice; RGRGE, red giant embryo glutinous rice; BR, black rice; BGRGE, black giant embryo glutinous rice. (For interpretation of the references to colour in this figure legend, the reader is referred to the web version of this article.)

were placed in a square container, into which a suitable volume of 0.304 mol/L potassium hydroxide solution was introduced. The container was then maintained in a 30 °C incubator for a period of 23 h, after which the extent of gelatinization of the endosperm in the rice grains was assessed.

Gel consistency was measured per the national standard “GB/T 22294-2008 Inspection of grain and oil-Determination of rice adhesive strength.” A precise quantity of 100 mg of processed rice flour was placed into a test tube, followed by the addition of 0.2 mL of 0.025 % methyl violet aqueous solution and 2.0 mL of 0.200 mol/L potassium hydroxide solution. The mixture was then thoroughly combined to facilitate gel formation. Subsequently, the distance that the gel flowed within the test tube was measured.

Amylose content was analyzed according to the spectrophotometric protocol outlined in “NY/T 2639-2014 Determination of amylose content in rice-Spectrophotometry method.” The iodine-blue colorimetric method (ISO 6647-2:2007) was employed for this measurement. A standard curve was created using standard samples with known amylose content, derived from their absorbance readings. The absorbance of the test sample was recorded at 620 nm, and the amylose content was calculated by applying the standard curve equation.

Protein was quantified via the automatic Kjeldahl nitrogen assessment procedure from “GB 5009.5-2016 Determination of protein in foods.”

2.4. Dry sample extraction

Representative brown rice samples from each variety—BGRGE, RGRGE, GRGE, BR, RR, GR, and WR—were subjected to UPLC-MS/MS analysis. Each rice accession was analyzed in three biological replicates. Biological samples were vacuum freeze-dried using a Scientz-100F lyophilizer, then ground into a fine powder with a Retsch MM 400 grinder at 30 Hz for 1.5 min. Approximately 50 mg of the powdered sample was extracted with 1200 µL of pre-cooled 70 % methanol containing an internal standard (Name: 2-chlorophenylalanine, Purity: 98 %, Concentration: 1 mg/L) at −20 °C. The mixture was vortexed for 0.5 min every 0.5 h, repeated six times. Samples were centrifuged (12,000 rpm, 3 mins), and the supernatant was filtered through a 0.22 µm microporous membrane before storage in injection vials for UPLC-MS/MS analysis.

2.5. UPLC conditions

The extracts were checked via UPLC-ESI-MS/MS system (UPLC: ExionLC™ AD, MS: Applied Biosystems 6500 Q TRAP, <https://sciex.com.cn/>). Specific process was as shown in Table 1.

2.6. ESI-q trap-MS/MS

ESI source parameters including 500 °C source temperature; 5500 V ion spray voltage for positive mode and −4500 V for negative mode; ion source gas I (GSI), gas II (GSII), and curtain gas (CUR) at 50, 60, and 25

Table 1
UPLC Conditions.

	Conditions/Processes
Chromatographic separation	Agilent SB-C18 (1.8 µm, 2.1 × 100 mm)
Solvent A	0.1 % formic acid in water
Solvent B	0.1 % formic acid in acetonitrile
Elution gradient program	95 % A + 5 % B, transitioning to 5 % A + 95 % B over 9 min, maintaining for one minute. The system then returned to 95 % A + 5 % B within 66 s and was kept for 174 s.
Flow rate and injection amount	The flow rate was 0.35 mL/min, with 40 °C column oven. The injection amount was 2 µL, and the effluent was directed to an ESI-triple quadrupole-linear ion trap (QTRAP)-MS.

psi, respectively; and collision-activated dissociation (CAD) set to high. MRM experiments were performed using nitrogen as the collision gas. Declustering potential (DP) and collision energy (CE) values were optimized for each MRM transition. Specific MRM transitions corresponding to metabolites eluted during defined periods were monitored.

2.7. PCA and hierarchical cluster analysis

Principal component analysis (PCA) was conducted using R (www.r-project.org), after scaling the data to unit variance. Hierarchical cluster analysis (HCA) results for samples and metabolites were visualized as heatmaps with dendrograms, while Pearson correlation coefficients (PCC) between samples were displayed as heatmaps. Both HCA and PCC analyses were conducted using the ComplexHeatmap package in R. Normalized metabolite intensities (scaled to unit variance) were colour-mapped for HCA visualization.

2.8. Identifying differential metabolites

Differential metabolites were identified based on variable importance in projection (VIP > 1) and absolute log2 fold change ($|\text{Log2FC}| \geq 1.0$). VIP score was used to assess the explanatory capacity and influence intensity of each compound on sample differentiation, with higher VIP scores indicating more significant differences in metabolic profiles between groups. VIP values were derived from OPLS-DA ($R^2Y = 1$, $p < 0.005$; $Q^2Y = 0.981$, $p < 0.005$) results, which included score and permutation plots generated using MetaboAnalystR. Data were log2-transformed and mean-centered before OPLS-DA. To minimize overfitting, a permutation test with 200 iterations was performed.

2.9. KEGG annotation and enrichment analysis

Metabolites were annotated using the KEGG Compound database (<http://www.kegg.jp/kegg/compound/>) and mapped to pathways in the KEGG Pathway database (<http://www.kegg.jp/kegg/pathway.html>). Enrichment analysis of significantly regulated pathways was performed using metabolite set enrichment analysis (MSEA). The significance of pathways was assessed using *p*-values derived from hypergeometric tests.

3. Results and discussion

3.1. Development of high nutrient-functional rice and evaluation of their quality traits

In recent years, rising living standards and economic improvements have led consumers to prioritize rice varieties that integrate taste, nutrition, and health benefits, fueling a growing demand for special rice. Consequently, the nutritional and functional properties of special rice have attracted significant research interest (Zhang et al., 2023; Zhao et al., 2024). Breeding efforts of special rice have shifted from focusing on single traits to multiple functional characteristics.

In this study, we developed 26 high nutrient-functional rice germplasms with unique traits, including colored seed coats, giant embryos, and glutinous characteristics, derived from the cross Heinuomi × Jupeixiangnuo. These included six black giant embryo glutinous rice (BGRGE), six red giant embryo glutinous rice (RGRGE), four giant embryo glutinous rice (GRGE), three black rice (BR), four red rice (RR) and three glutinous rice (GR). Additionally, three white rice (WR) germplasms were created using the same parents (Fig. 1).

We evaluated the appearance, milling, cooking, and nutritional qualities of the different brown rice types. Grain length ranged from 7.54 to 8.85 mm, classifying them as long grain, while grain width varied from 3.32 to 4.31 mm (Fig. 2 and Table S1). The length-to-width ratio ranged from 2.03 to 2.53, with GR and GRGE classified as broad ovoid-shaped (ratios of 2.03 and 2.11, respectively). Other brown rice

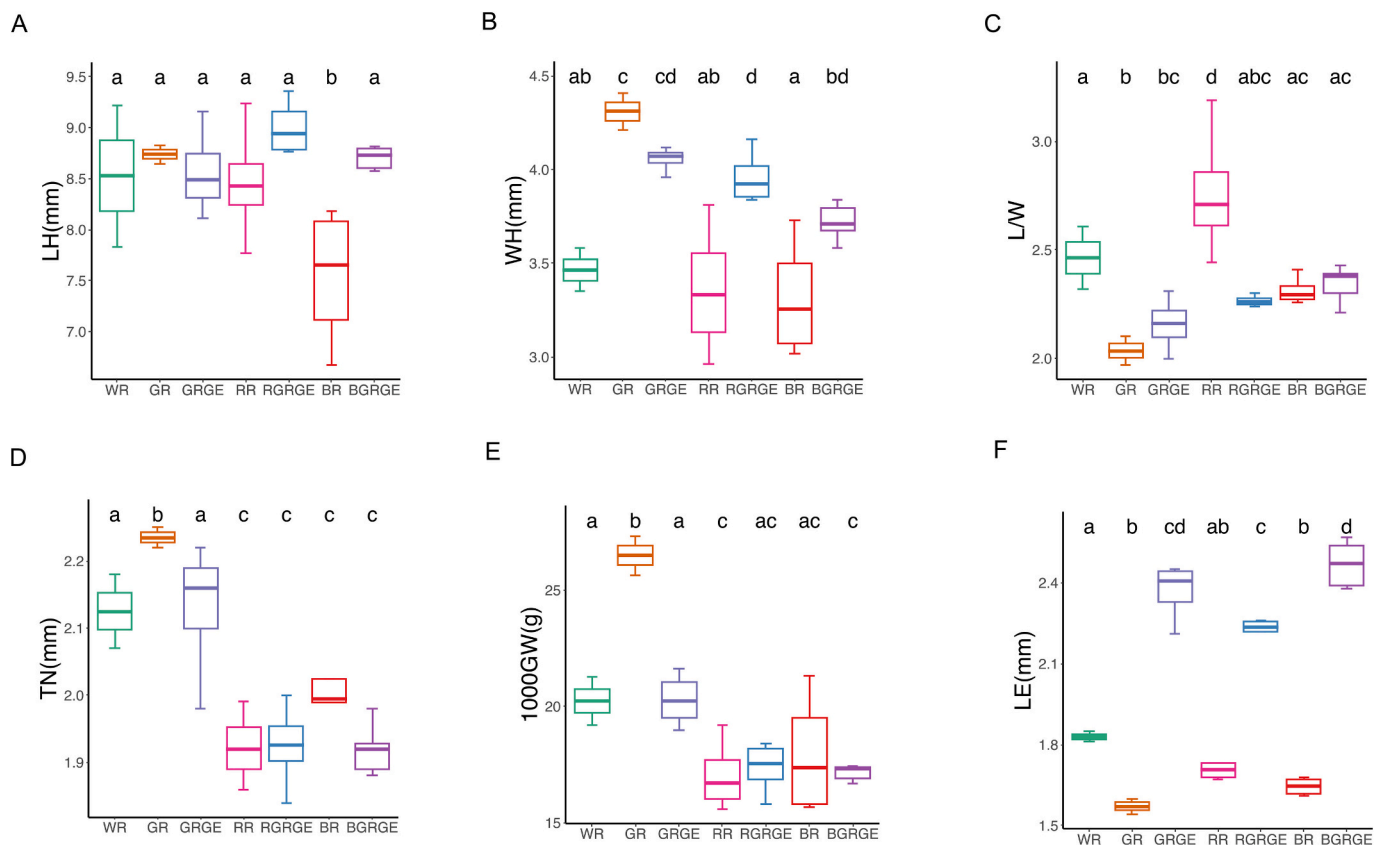


Fig. 2. Phenotypic variation across different special rice. (A-F): LH, grain length; WH, grain width; L/W, length-to-width ratio; TN, grain thickness; 1000GW, 1000-grain weight; LE, embryo length. Different letters above the boxes indicate significant differences ($p < 0.05$, Bonferroni correction) in multiple comparison testing.

types were categorized as oval-shaped, with ratios between 2.26 and 2.51. Thickness varied from 1.92 mm to 2.24 mm, with RR, BGRGE, and RGRGE being thinner (< 2 mm), significantly less than WR ($p < 0.05$). The 1000-grain weight ranged from 17.05 to 26.48 g, with RR, BGRGE, RGRGE, and BR weighing 84.3–88.6 % of WR. Embryo length varied significantly, from 1.57 mm to 2.43 mm. Notably, BGRGE, RGRGE, and GRGE exhibited the longest embryos, measuring 122.9–132.5 % of WR, which indicated they might contained more physiologically active compounds in their embryos than WR, such as GABA, amino acid, vitamins, etc.

The head rice rate ranged from 25.4 % (RR) to 60.2 % (GR). Alkali spreading values were consistent at 7, except for RR. GR, BGRGE, RGRGE, and GRGE showed higher gel consistency (95–100 mm) and lower amylose content (0.2–0.5 %). Protein content ranged from 7.0 % to 8.8 %, with GR, BGRGE, RGRGE, and GRGE lower than WR (Table S2).

3.2. Metabolic profiling of the brown rice

Comprehensive metabolic profiling of representative BGRGE, RGRGE, GRGE, BR, RR, GR, and WR was performed using UPLC-MS/MS. A total of 1347 metabolites were identified, including flavonoids (223, 16.56 %), lipids (181, 13.44 %), amino acids and derivatives (170, 12.62 %), phenolic acids (162, 12.03 %), alkaloids (138, 10.24 %), terpenoids (91, 6.76 %), organic acids (84, 6.24 %), nucleotides and derivatives (66, 4.90 %), lignans and coumarins (29, 2.15 %), quinones (16, 1.19 %), tannins (3, 0.22 %), steroids (1, 0.07 %), and others (183, 13.59 %) (Fig. 3A and Table S3). This represents nearly double the number of metabolites identified in prior studies (Zhang et al., 2023), providing a rich dataset for isolating and characterizing functional compounds in rice grains.

Amino acids and vitamins are essential components of rice

nutritional quality. To explore the variations in the characteristics of amino acids and vitamins in different special rice, we examined the relative contents of essential amino acids and vitamins B (B2, B3, B5 and B13). As shown in Fig. S1, we found that L-Phenylalanine ($\text{Log}_2\text{FC} = 1.72$), Vitamin B2 ($\text{Log}_2\text{FC} = 4.16$) and Vitamin B13 ($\text{Log}_2\text{FC} = 2.15$) had highest relative contents in BGRGE, which showed all significantly higher relative contents than that in WR ($p < 0.05$). L-Valine and L-Lysine had highest relative contents in GRGE, and the relative contents of L-Lysine in GRGE is 2.18 times as much as that in WR ($p < 0.05$). Additionally, L-Leucine, L-Isoleucine, L-Tryptophan and DL-Methionine had highest relative contents in RR. These results indicated some amino acids and vitamins are more abundant in special rice.

Multivariate statistical analysis revealed significant metabolite differentiation among the seven groups. Principal Component Analysis (PCA) showed distinct separation, with the first principal component (PC1) (29.12 %) and second principal component (PC2) (19.32 %) explaining 48.44 % of the total variance (Fig. 3B). PC1 differentiated giant embryo varieties (BGRGE, RGRGE, GRGE) from non-giant embryo types (BR, RR, GR, WR), while PC2 separated pigmented (BGRGE, RGRGE, BR, RR) from non-pigmented rice (GRGE, GR, WR).

Hierarchical cluster analysis (HCA) revealed eight main clusters of metabolite accumulation patterns (Fig. 3C). Cluster I metabolites were highly abundant in RGRGE, while clusterII metabolites dominated in BGRGE. Clusters III, IV, VI, VII, and VIII showed the highest accumulation in GRGE, GR, BR, RR, and WR, respectively. The HCA results aligned with PCA findings, confirming clear metabolic distinctions among the seven rice groups, and highlighting significant metabolite variation. Interestingly, we found flavonoids were highly abundant in pigmented rice (BGRGE, RGRGE, BR, RR), which separated pigmented from non-pigmented rice (GRGE, GR, WR). Lipids showed the higher accumulation in GR and GRGE (Fig. S2). Previous studies have reported that the content of lipids were significantly increased in waxy corn

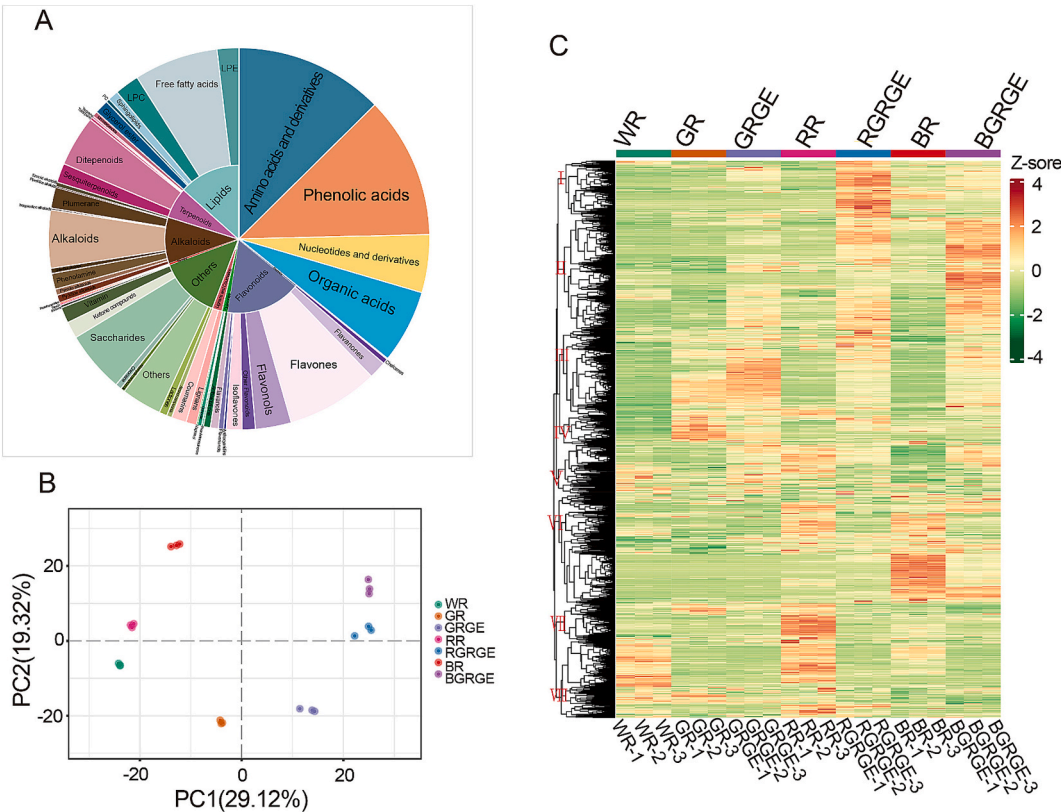


Fig. 3. Classification, principal component analysis (PCA), and hierarchical cluster analysis (HCA) of metabolic profiles in special rice. (A) Classification of 1347 metabolites in brown rice samples. (B) PCA score plot of metabolites. (C) HCA heatmap of metabolites, with each column representing a sample and each row representing a metabolite. Red indicates higher metabolite abundance, while green indicates lower abundance. (For interpretation of the references to colour in this figure legend, the reader is referred to the web version of this article.)

kernels (Li et al., 2025), and our study confirmed this finding. Amino acids and derivatives were enriched in GRGE, RGRGE, and BGRGE. Given that amino acids are primarily synthesized and accumulated in the embryo, the development of giant embryo rice is beneficial for enhancing the content of amino acids. Terpenoids, which were well known for their antioxidant, anti-inflammatory, and immunomodulatory properties, were unexpectedly found at higher levels in BGRGE. This highlighted the potential value of BGRGE and it was worth to in-depth study its metabolic mechanism and utilize in high-nutrient functional rice breeding.

3.3. Differential metabolites among different types of special rice

The comprehensive metabolite dataset generated in this study offers valuable insights into the differential metabolites across various specialty rice types. We compared GR and GRGE to explore the metabolite characteristics of giant embryo rice. This analysis identified 204 differential metabolites, categorized into 11 distinct groups (Fig. 4 and Table S4). Compared to GR, GRGE exhibited 168 upregulated metabolites, mainly including 37 aa and derivatives, 15 organic acids (such as γ -Aminobutyric acid), 31 phenolic acids, and 22 alkaloids. Conversely, 36 metabolites were downregulated in GRGE, namely 16 flavonoids, five phenolic acids, and

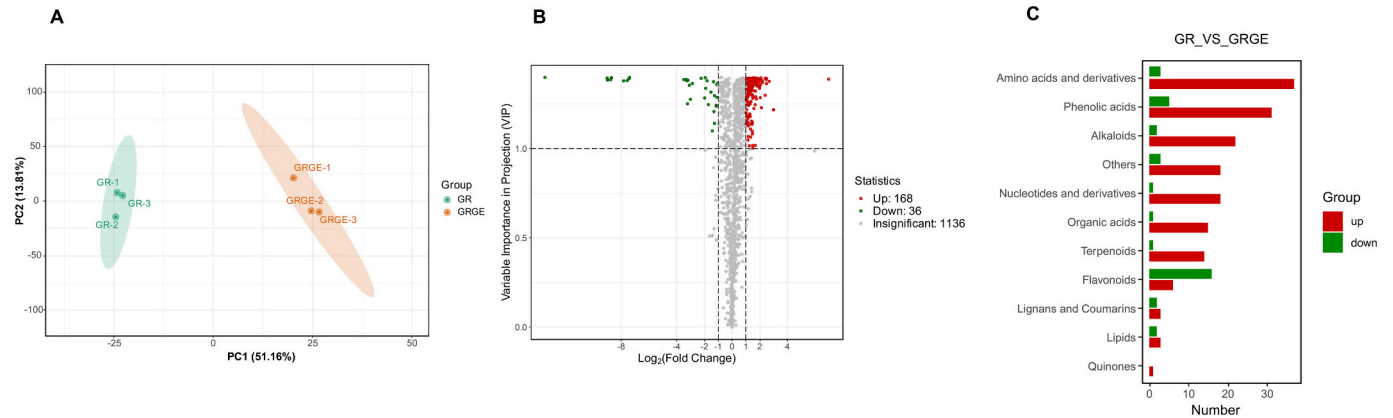


Fig. 4. Analysis of differential metabolites between GR and GRGE groups. (A) OPLS-DA score plots. (B) Volcano plot showing differential metabolite expression levels between GR vs GRGE. (C) Classification of differential metabolites. GR, glutinous rice; GRGE, giant embryo glutinous rice.

three aa and derivatives, etc. These results indicate significant metabolite differences between GR and GRGE, with GRGE enriched in γ -aminobutyric acid, amino acids and derivatives, and other physiologically active substances and nutrients. Notably, GRGE had significantly higher relative contents of GABA than GR (VIP = 1.39, Log2FC = 1.93), and the relative contents of GABA in GRGE is 3.81 times as much as that in GR. GABA is known for its health benefits, including enhancing liver and kidney function, promoting insulin secretion, and supporting diabetes management (Huang et al., 2014). Additionally, GABA has been associated with lowering blood pressure and lipids, preventing arteriosclerosis and obesity, regulating arrhythmias, and combating fatigue and aging. These properties have earned giant embryo rice the nickname “longevity rice” (Hu et al., 2022).

We identified differential metabolites in comparison groups (WR vs BR/RR) (Fig. 5A-D and Table S5–6). In this analysis, a total of 343 metabolites were upregulated in BR compared to WR, mainly including 124 flavonoids (such as anthocyanidins), 76 phenolic acids, 23 alkaloids, 22 terpenoids, 14 aa and derivatives, and 13 lipids. Conversely, 83 metabolites were downregulated in BR, consisting of 33 flavonoids, 11 alkaloids, eight phenolic acids, and six aa and derivatives, etc. In RR, 298 metabolites were upregulated relative to WR, mainly including 115 flavonoids, 48 phenolic acids, 34 alkaloids, 24 amino acids and derivatives, 16 lipids, and three terpenoids. Additionally, 43 metabolites were downregulated in RR, namely 10 terpenoids, nine phenolic acids, eight alkaloids, and five lipids, etc. Notably, 214 metabolites exhibited upregulation in both types of pigmented rice, whereas 10 metabolites

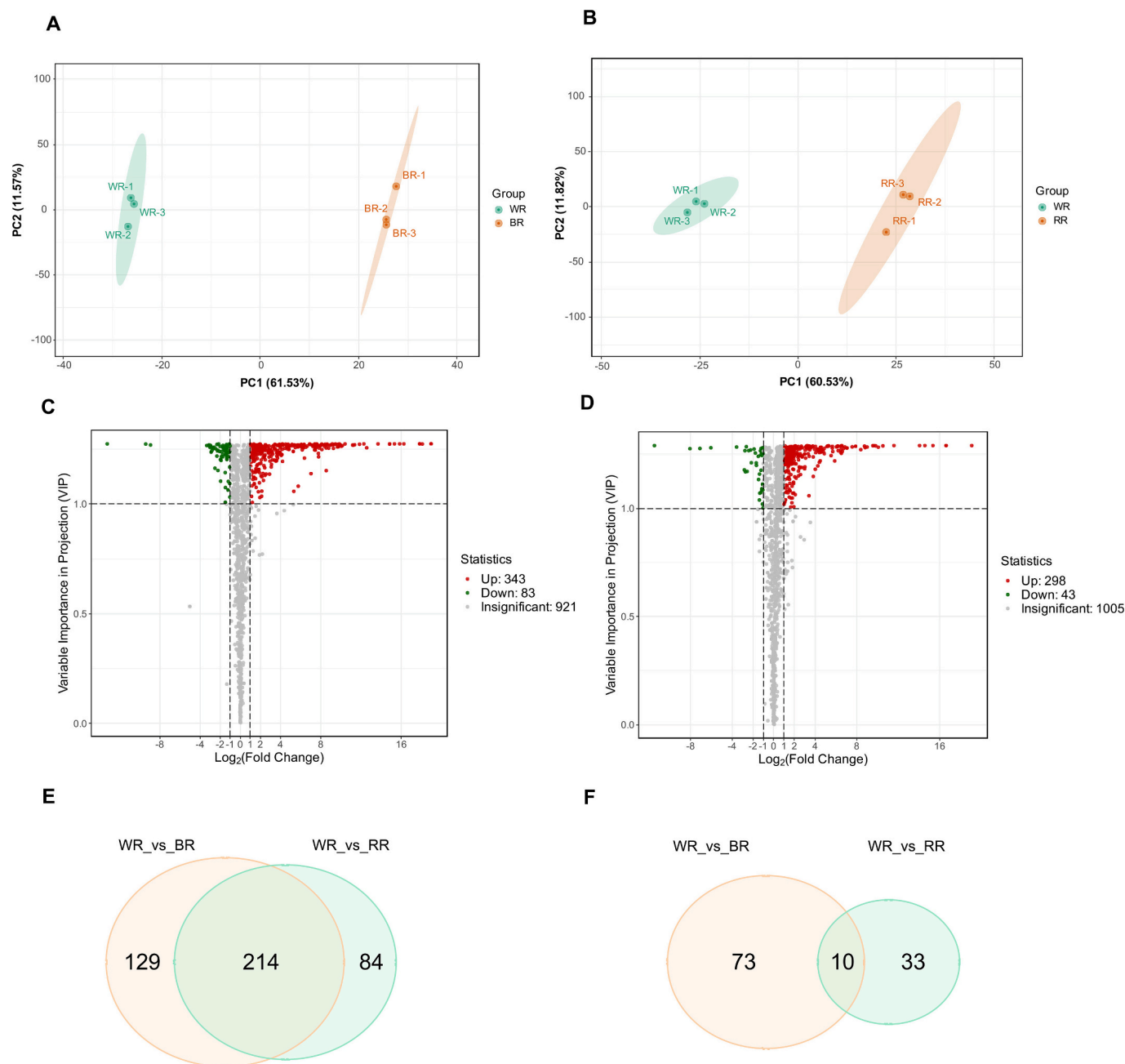


Fig. 5. Analysis and comparison of differential metabolites in pigmented brown rice (BR and RR) vs. non-pigmented brown rice (WR). (A–B) OPLS-DA score plots for WR vs. BR (A) and WR vs. RR (B). (C–D) Volcano plots showing differential metabolite expression levels for WR vs. BR (C) and WR vs. RR (D). (E) Venn diagram of overlapping and unique up-regulated differential metabolites in WR vs. BR and WR vs. RR. (F) Venn diagram of overlapping and unique down-regulated differential metabolites in WR vs. BR and WR vs. RR. (For interpretation of the references to colour in this figure legend, the reader is referred to the web version of this article.)

showed downregulation across both (Fig. 5E–F). Flavonoids account for 44.4 % of the shared upregulated metabolites, indicating that flavonoid profiles differ significantly across pigmented and non-pigmented rice.

Black rice is renowned for its high content of bioactive compounds, such as flavonoids (anthocyanins) (Chen, Tao, et al., 2019), phenols (Ding et al., 2019; Ziegler et al., 2018), and terpenoids (Kim et al., 2021). Among them, flavonoids can combine with peroxide radicals to form relatively stable flavonoid radicals due to the hydrogen atoms on the phenolic hydroxyl group, which then react with other free radicals, thereby terminating the free radical chain reaction and playing a role in eliminating free radicals, antioxidation, and anti-aging (Shen, Jin, Xiao, Lu, & Bao, 2009).

Additionally, the compounds in black rice confer medicinal properties, such as lipid-lowering effects (Wang et al., 2020), and cholesterol reduction. Hence, black rice is often considered a “medicinal food” rice. Red rice contains bioactive components similar to black rice, especially phenols and terpenes but at distinct concentrations, which conferred unique medicinal functions properties such as antioxidant, anti-inflammatory, and lipid-lowering effects (Kim et al., 2021; Praphasawat et al., 2023; Ziegler et al., 2018). Our findings corroborate these properties, with BR showing elevated levels of 343 metabolites, mainly including 124 flavonoids, 76 phenolic acids, 22 terpenoids, 14 lignans and coumarins. RR was similar with BR, showing elevated levels of 298

metabolites, which underscore BR and RR as excellent candidates for dietary therapy to prevent or manage chronic diseases.

To obtain a comprehensive understanding of metabolite features in colored giant embryo rice, we identified differential metabolites across four groups (GR/WR vs. BGRGE and GR/WR vs. RGRGE) (Fig. 6A and Table S7–10). This analysis uncovered 482 significantly different metabolites across GR vs. BGRGE (421 upregulated and 61 downregulated), 629 between WR vs. BGRGE (527 upregulated and 102 downregulated), 437 between GR vs. RGRGE (396 upregulated and 41 downregulated), and 602 between WR vs. RGRGE (514 upregulated and 88 downregulated). Differential metabolites in the four groups were classified into 12, 13, 12, and 13 distinct categories (Fig. 6B–E and Tables S7–S10). Secondary metabolites (e.g., flavonoids, phenolic acids, alkaloids, terpenoids, and lignans) constituted over 60 % of the differential metabolites. Flavonoid metabolite profiles exhibited variability between GR/WR and BGRGE/RGRGE. Furthermore, we uncovered differential metabolites, including organic acids (such as γ -Aminobutyric acid), vitamins, lipids, nucleotides and derivatives, as well as aa and derivatives. Venn diagram analysis indicates that 264 metabolites were upregulated in both classes of pigmented giant embryo rice, including flavonoids, organic acids (such as γ -Aminobutyric acid), and vitamins, whereas five metabolites were downregulated (Fig. 6F–G).

This metabolic profile establishes pigmented giant embryo rice as a

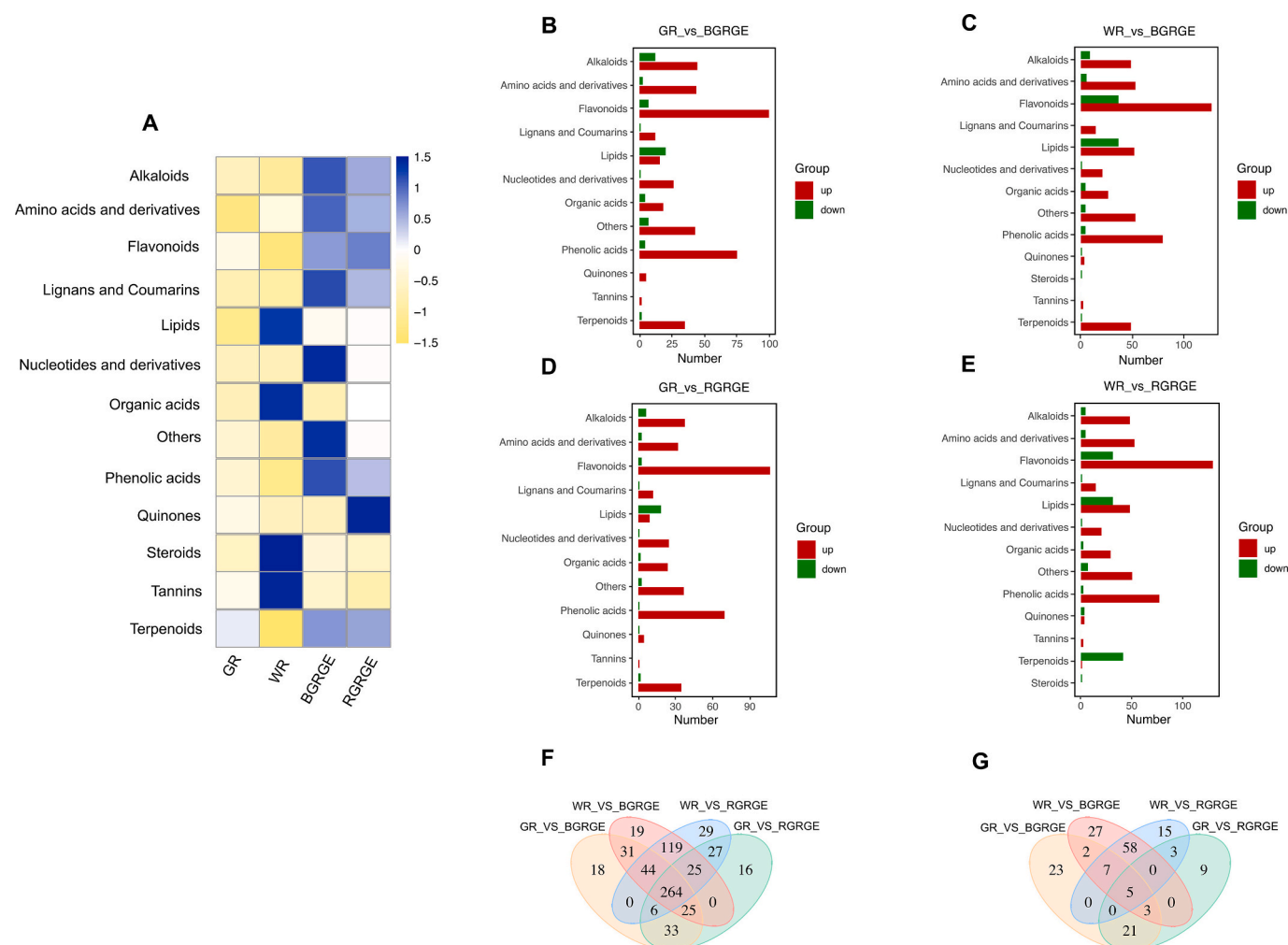


Fig. 6. (A) Accumulation patterns of differential metabolite classes in various rice grains. (B–E) Classification of differential metabolites. WR, white rice; GR, glutinous rice; BGRGE, black giant embryo glutinous rice; RGRGE, red giant embryo glutinous rice. (F) Venn diagram of overlapping and unique up-regulated differential metabolites across four comparison groups (WR vs. BGRGE, GR vs. BGRGE, WR vs. RGRGE, and GR vs. RGRGE). (G) Venn diagram of overlapping and unique down-regulated differential metabolites for the same comparison groups (WR vs. BGRGE, GR vs. BGRGE, WR vs. RGRGE, and GR vs. RGRGE). (For interpretation of the references to colour in this figure legend, the reader is referred to the web version of this article.)

highly valuable functional food with considerable market potential, which combines the physiologically active substances and nutrients of both giant embryo rice and pigmented rice, enriched in γ -aminobutyric acid, anthocyanidins, vitamins, and amino acids and derivatives. In future special rice breeding, it is recommended to combine two or more desirable traits, such as colored seed coat, giant embryo, and glutinous characteristics to meet the diverse consumer demands for nutritional and functional rice. The 26 newly developed special rice germplasms in this study can be directly used as parental lines for special rice breeding of high function and nutritional quality. Additionally, they also can be used as raw materials for the development of nutritional and functional foods, such as rice noodles, rice wine, rice cakes, etc.

3.4. KEGG enrichment analysis of differential metabolites

Differential metabolites from WR/GR vs. BGRGE and WR/GR vs. RGRGE groups were enriched in the KEGG pathways, associated with 83, 75, 83, and 71 pathways, respectively. Primary pathways are presented in bubble plots (Fig. S3A–D). When comparing WR vs. BGRGE (Table S11), metabolic pathways related to flavonoid biosynthesis, flavone and flavonol biosynthesis, and secondary metabolite biosynthesis were significantly enriched ($p < 0.05$). When comparing GR vs. BGRGE (Table S12), significant enrichment was identified in pathways linked to flavonoid biosynthesis, biosynthesis of cofactors, biosynthesis of secondary metabolites, tyrosine metabolism, and tryptophan metabolism ($p < 0.05$). For WR vs. RGRGE comparison (Table S13), significant enrichment was identified in metabolic pathways, including the

biosynthesis of flavonoid, flavone, flavonol, and secondary metabolite, as well as the tryptophan metabolism ($p < 0.05$). In the GR vs. RGRGE comparison (Table S14), riboflavin metabolism, flavonoid biosynthesis, starch and sucrose metabolism, and secondary metabolite biosynthesis were significantly enriched ($p < 0.05$). Overall, differential metabolites between WR/GR vs. BGRGE/RGRGE were involved in various critical pathways, with significant enrichment in the biosynthesis of flavone, flavonol, flavonoid, and secondary metabolite ($p < 0.05$), which was consistent with previous studies that identified the flavonoid pathway as prominently regulated among different pigmented rice types (Sudan et al., 2023; Zheng et al., 2021; Zhang et al., 2023; Xia et al., 2023; Chen, Tao, et al., 2019; Chen, Zhou, et al., 2019; Zhao et al., 2024).

To facilitate an overview of the key major differentially regulated pathways between WR/GR and BGRGE/RGRGE, we constructed a diagram based on KEGG maps of flavonoid biosynthesis (Fig. 7). The key differential metabolites in flavonoid biosynthesis include pinobanksin (BGRGE: $\text{Log}_2\text{FC} = 7.29$; RGRGE: $\text{Log}_2\text{FC} = 5.42$), hesperetin (BGRGE: $\text{Log}_2\text{FC} = 6.40$; RGRGE: $\text{Log}_2\text{FC} = 6.64$), butin (BGRGE: $\text{Log}_2\text{FC} = 7.05$; RGRGE: $\text{Log}_2\text{FC} = 5.21$), naringenin chalcone (BGRGE: $\text{Log}_2\text{FC} = 6.78$; RGRGE: $\text{Log}_2\text{FC} = 4.99$), naringenin (BGRGE: $\text{Log}_2\text{FC} = 7.28$; RGRGE: $\text{Log}_2\text{FC} = 5.47$), homoeriodictyol (BGRGE: $\text{Log}_2\text{FC} = 7.08$; RGRGE: $\text{Log}_2\text{FC} = 7.97$), eriodictyol (BGRGE: $\text{Log}_2\text{FC} = 8.17$; RGRGE: $\text{Log}_2\text{FC} = 6.75$), tricetin (BGRGE: $\text{Log}_2\text{FC} = 7.55$; RGRGE: $\text{Log}_2\text{FC} = 8.51$), myricetin (BGRGE: $\text{Log}_2\text{FC} = 4.21$; RGRGE: $\text{Log}_2\text{FC} = 7.08$), quercetin (BGRGE: $\text{Log}_2\text{FC} = 6.53$; RGRGE: $\text{Log}_2\text{FC} = 4.56$), dihydrokaempferol (BGRGE: $\text{Log}_2\text{FC} = 4.62$; RGRGE: $\text{Log}_2\text{FC} = 3.59$), and dihydroquercetin (BGRGE: $\text{Log}_2\text{FC} = 6.50$; RGRGE: $\text{Log}_2\text{FC} = 8.33$). These metabolites

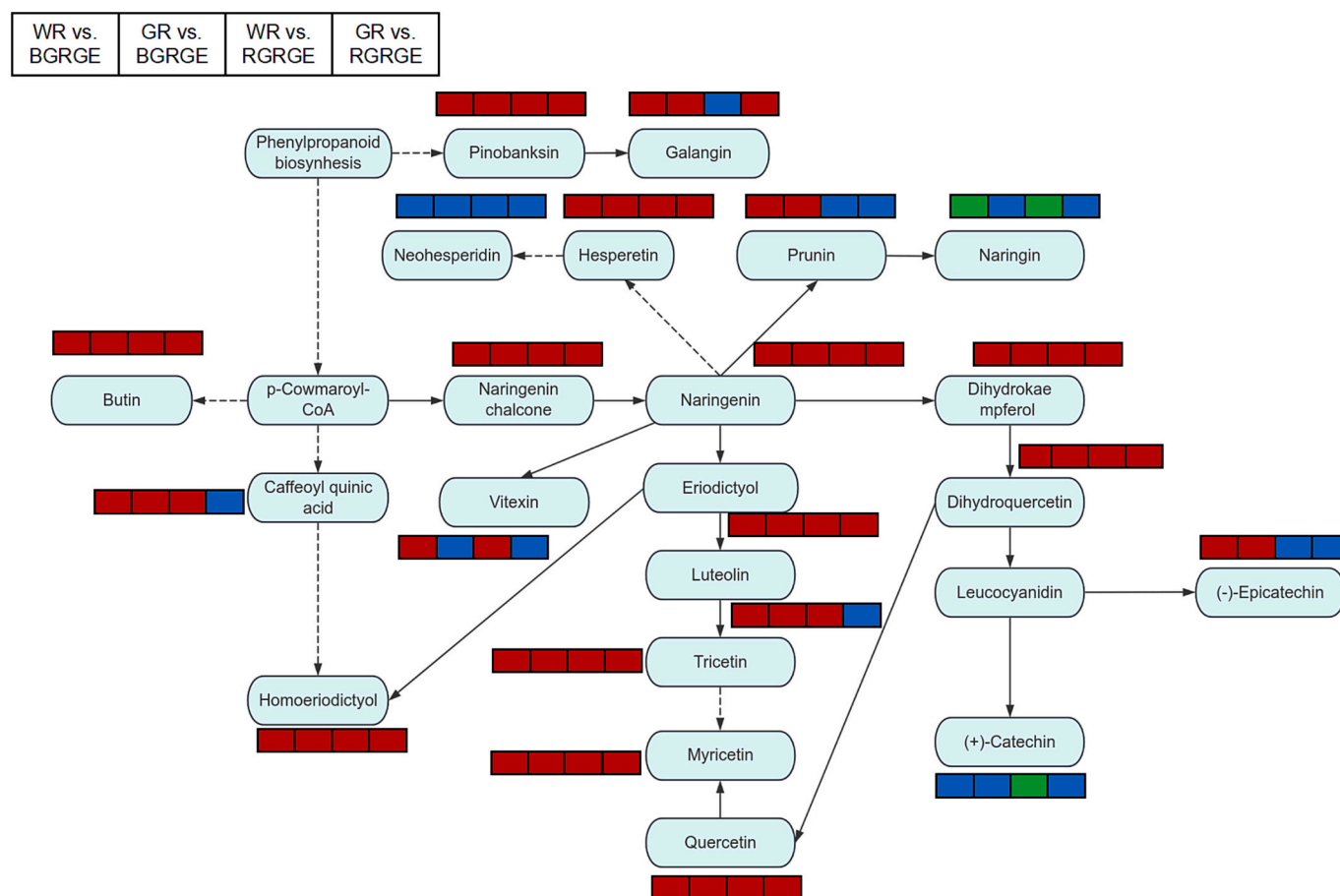


Fig. 7. Overview of the probable regulation of certain key metabolites mapped to metabolic pathways of flavonoid biosynthesis in pairwise comparisons between WR/GR and BGRGE/RGRGE. Note: The green and red rectangles, respectively, indicate that the metabolite content is significantly down-regulated and up-regulated; the blue rectangle indicates no significant difference. (For interpretation of the references to colour in this figure legend, the reader is referred to the web version of this article.)

were all upregulated in both BGRGE and RGRGE, which indicated they played an important role in enhancing biological activity in flavonoid.

To further elucidate the molecular mechanisms underlying these traits, a multi-omics approach integrating gene expression analysis and metabolomics across different rice types will be necessary. This will provide a comprehensive understanding of the variation in rice nutritional quality and dissect the molecular regulatory networks driving these differences.

4. Conclusions

This study utilized UPLC-MS/MS-based widely targeted metabolomics to identify and analyze the diverse metabolites in various types of special rice. This comprehensive approach elucidated the metabolite variation among rice types, highlighting the accumulation patterns of key nutraceuticals and unique metabolite distribution characteristics of each variety. Giant embryo rice was identified as a rich source of γ -Aminobutyric acid, vitamins, amino acids, and other bioactive compounds, reinforcing its potential as a vital ingredient for disease prevention and therapeutic applications. Similarly, black and red rice exhibited exceptional levels of flavonoids, phenolic acids, terpenoids, and alkaloids, further affirming their functional and medicinal properties. Notably, pigmented giant embryo rice combined the physiologically active substances and nutrients of both pigmented rice and giant embryo rice, establishing it as an exceptional functional rice with significant market potential. Key differential metabolic pathways included flavone, flavonol, flavonoid, and secondary metabolite production, offering critical insights into the metabolic mechanisms driving the unique traits of special rice. This study provides a detailed metabolite profile of diverse specialty rice types, enhancing our understanding of their nutritional and functional value.

CRedit authorship contribution statement

Di Cui: Writing – original draft, Methodology, Investigation, Data curation. **Zichao Zhu:** Investigation, Formal analysis. **Soon-Wook Kwon:** Software, Methodology, Funding acquisition. **Joohyun Lee:** Software, Resources. **Mingmao Sun:** Visualization, Resources, Methodology. **Xiaodong Ma:** Validation, Resources, Investigation. **Chutao Wang:** Resources, Investigation. **Bing Han:** Resources, Investigation. **Xianying Li:** Project administration, Funding acquisition. **Longzhi Han:** Writing – review & editing, Supervision, Resources, Methodology, Funding acquisition, Conceptualization.

Declaration of competing interest

The authors declare that they have no known competing financial interests or personal relationships that could have appeared to influence the work reported in this paper.

Acknowledgements

This work was supported by Strategic Cooperation Project of Agricultural Science and Technology Innovation between Chongqing Municipal People's Government and Chinese Academy of Agricultural Sciences, the National Natural Science Foundation of China (32201765), the National Research Foundation of Korea (NRF) grant funded by the Korea government (No. RS-2024-00391988), Key Research and Development Program of Shandong Province of China (2019GNC106107), the National Key Research and Development Program of China (2021YFD1200500), the CAAS Science and Technology Innovation Program.

Appendix A. Supplementary data

Supplementary data to this article can be found online at <https://doi.org/10.1016/j.fochx.2025.102890>.

[org/10.1016/j.fochx.2025.102890](https://doi.org/10.1016/j.fochx.2025.102890).

Data availability

Data will be made available on request.

References

- Battaglioli, G., Liu, H., & Martin, D. L. (2003). Kinetic differences between the isoforms of glutamate decarboxylase: Implications for the regulation of GABA synthesis. *Journal of Neurochemistry*, 86(4), 879–887. <https://doi.org/10.1046/j.1471-4159.2003.01876.x>
- Chen, X., Tao, Y., Ali, A., Zhuang, Z., Guo, D., Guo, Q., ... Wu, X. (2019). Transcriptome and proteome profiling of different colored rice reveals physiological dynamics involved in the flavonoid pathway. *International Journal of Molecular Sciences*, 20, 2463. <https://doi.org/10.3390/ijms20102463>
- Chen, X., Zhou, X., Yang, Z., Gu, C., Tao, Y., Guo, Q., ... Wu, X. (2019). Analysis of quality involving minerals, amylose, protein, polyphenols and antioxidant capacity in different coloured rice varieties. *Food Science and Technology Research*, 25(1), 141–148. <https://doi.org/10.3136/fstr.25.141>
- Determination of amylose content in rice-Spectrophotometry method. NY/T 2639-2014 [S]. 2014.
- Determination of protein in foods. GB 5009.5-2016[S]. 2016.
- Determination of rice quality. NY/T 83-2017[S]. 2017.
- Ding, C., Liu, Q., Li, P., Pei, Y., Tao, T., Wang, Y., ... Shao, X. (2019). Distribution and quantitative analysis of phenolic compounds in fractions of japonica and Indica rice. *Food Chemistry*, 274, 384–391. <https://doi.org/10.1016/j.foodchem.2018.10.055>
- Hu, M. M., Lan, Y., Peng, L. G., Li, C. M., Chen, G. Y., Kuang, H. D., ... Li, T. (2022). Effects of nitrogen application rate on yield, quality, and γ -aminobutyric acid content of giant embryo rice. *Journal of Plant Nutrition and Fertilizers*, 28(11), 1947–1963. <https://doi.org/10.11674/zwfy.2022163>
- Hu, P. S. (2003). Research and development of functional rice. *China Rice*, 5, 3–5. <https://doi.org/10.3969/j.issn.1006-8082.2003.05.001>
- Hu, S. K., & Hu, P. S. (2021). Current status and prospects of functional rice. *Research. China Rice Science*, 35(4), 311–325. <https://doi.org/10.16819/j.1001-7216.2021.201106>
- Huang, C. Y., Kuo, W. W., Wang, H. F., Lin, C. J., Lin, Y. M., Chen, J. L., ... Lin, J. Y. (2014). GABA tea ameliorates cerebral cortex apoptosis and autophagy in streptozotocin-induced diabetic rats. *Journal of Functional Foods*, 6, 534–544. <https://doi.org/10.1016/j.jff.2014.02.007>
- Inspection of grain and oil-Determination of rice adhesive strength. GB/T 22294-2008 [S]. 2008.
- Kim, K. H., Heu, M. H., & Park, S. Z. (1991). New mutants for rice grain. Quality. *The Korean Journal of Crop Science*, 36, 197–203. <https://doi.org/10.3321/j.issn:0578-1752.2007.03.001>
- Kim, T. J., Kim, S. Y., Park, Y. J., Lim, S. H., Ha, S. H., Park, S. U., ... J. K. (2021). Metabolite profiling reveals distinct modulation of complex metabolic networks in non-pigmented, black, and red rice (*Oryza sativa* L. cultivars). *Metabolites*, 11(6), Article 3674. <https://doi.org/10.3390/metabol11.06.3674>
- Koh, H. J., Heu, M. H., & McCouch, S. R. (1996). Molecular mapping of the ges. Gene controlling the super-giant embryo character in rice (*Oryza sativa* L.). *Theoretical and Applied Genetics*, 93, 257–261. <https://doi.org/10.1007/s001220050274>
- Li, C., Li, Z., Lu, B., Shi, Y., Xiao, S., Dong, H., ... Zhao, J. (2025). Large-scale metabolomic landscape of edible maize reveals convergent changes in metabolite differentiation and facilitates its breeding improvement. *Molecular Plant*, 18(4), 619–638. <https://doi.org/10.1016/j.molp.2025.02.007>
- Liu, L. L., Jiang, L., & Liu, S. J. (2005). Changes in γ -aminobutyric acid. Content of super-giant rice W025 brown rice after soaking. *Acta Agronomica Sinica*, 31(10), 23–28. <https://doi.org/10.3321/j.issn:0496-3490.2005.10.004>
- Mau, J.-L., Lee, C.-C., Chen, Y.-P., & Lin, S.-D. (2017). Physicochemical, antioxidant and sensory characteristics of chiffon cake prepared with black rice as replacement for wheat flour. *LWT - Food Science and Technology*, 75, 434–439. <https://doi.org/10.1016/j.lwt.2016.09.019>
- Prapthasawat, R., Palipoch, S., Suwannaler, P., Payuhakrit, W., Kunsorn, P., Laovithayangoon, S., ... Klajing, W. (2023). Red rice bran extract suppresses colon cancer cells via apoptosis induction/cell cycle arrest and exerts antimutagenic activity. *Experimental Oncology*, 45(2), 220–230. <https://doi.org/10.32592/eo.2023.45.2.220>
- Shen, Y., Jin, L., Xiao, P., Lu, Y., & Bao, J. (2009). Total phenolics, flavonoids, antioxidant capacity in rice grain and their relations to grain color, size and weight. *Journal of Cereal Science*, 49(1), 106–111. <https://doi.org/10.1016/j.jcs.2008.07.007>
- Su, N., Wan, X. Y., Zhai, H. Q., & Wan, J. M. (2007). Current status and trends in. *Research on functional rice. China. Agricultural Sciences*, 40(3), 433–439.
- Sudan, J., Urwat, U., Farooq, A., Pakhtoon, M. M., Zaffar, A., Naik, Z. A., ... Zargar, S. M. (2023). Explicating genetic architecture governing nutritional quality in pigmented rice. *PeerJ*, 11, Article e15901. <https://doi.org/10.7717/peerj.15901>
- Tang, Y., Cai, W., & Xu, B. (2016). From rice bag to table: Fate of phenolic. Chemical compositions and antioxidant activities in waxy and non-waxy black rice during home cooking. *Food Chemistry*, 191, 81–90. <https://doi.org/10.1016/j.foodchem.2015.02.001>
- Wang, H., Liu, D., Ji, Y., Liu, Y., Xu, L., & Guo, Y. (2020). Dietary. Supplementation of black rice anthocyanin extract regulates cholesterol metabolism and improves gut microbiota dysbiosis in C57BL/6J mice fed a high-fat and cholesterol diet. *Molecular*

- Nutrition & Food Research*, 64(8), Article 1900876. <https://doi.org/10.1002/mnfr.201900876>
- Xia, H., Pu, X., Zhu, X., Yang, X., Guo, H., Diao, H., ... Zhang, Z. (2023). Genome-wide association study reveals the genetic basis of total flavonoid content in brown rice. *Genes*, 14, 1684. <https://doi.org/10.3390/genes14081684>
- Zhang, L., Cui, D., Ma, X., Han, B., & Han, L. (2023). Comparative analysis of. Rice reveals insights into the mechanism of colored rice via widely targeted metabolomics. *Food Chemistry*, 399, Article 133926. <https://doi.org/10.1016/j.foodchem.2022.133926>
- Zhang, X. X., Yuan, L. F., Luo, L. G., Zhang, B. J., Xiong, Y., Wu, L., ... Tu, T. H. (2019). Breeding and application of a new variety of indica super-giant functional rice "black pearl". *Journal of Jiangxi Agricultural Sciences*, 31(5), 6–10. <https://doi.org/10.3969/j.issn.1001-8581.2019.05.002>
- Zhao, M., Huang, J., Ren, J., Xiao, X., Li, Y., Zhai, L., ... Tang, Q. (2024). Metabolomic insights into primary and secondary metabolites variation in common and glutinous rice (*Oryza sativa* L.). *Agronomy*, 14, 1383. <https://doi.org/10.3390/agronomy14061383>
- Zheng, J., Wu, H., Zhao, M., Yang, Z., Zhou, Z., Guo, Y., ... Chen, H. (2021). OsMYB3 is a R2R3-MYB gene responsible for anthocyanin biosynthesis in black rice. *Molecular Breeding*, 41, 51. <https://doi.org/10.1007/s11032-021-01165-5>
- Ziegler, V., Ferreira, C. D., Hoffmann, J. F., Chaves, F. C., Vanier, N. L., Oliveira, M., & Elias, M. C. (2018). Cooking quality properties and free and bound phenolics content of brown, black, and red rice grains stored at different temperatures for six months. *Food Chemistry*, 242, 427–434. <https://doi.org/10.1016/j.foodchem.2017.09.060>